Two-Dimensional Potential Flow Theory for Multiple Bodies in Small Amplitude Motion

JOSEPH P. GIESING*
McDonnell Douglas Corporation, Long Beach, Calif.

This paper describes a very general method for determining the unsteady, two-dimensional, incompressible flow about one or more bodies of arbitrary shape. Specifically the surface pressure, forces and moments are obtained for bodies oscillating with small amplitude about their steady equilibrium position and on bodies in small amplitude gust fields. The equilibrium configuration of the bodies may also be arbitrary. Calculated results for single bodies in and out of gust fields are compared to results obtained by existing methods. Calculations and comparisons are also presented for two interacting bodies.

Nomenclature

A_{lm} = complex velocity (normal—i tangential) at the midpoint of element l due to element m of unit source strength
AI = imaginary part of A
AR = real part of A
C_p = $p - p_\infty/\frac{1}{2}\rho_\infty U_\infty^2$ pressure coefficient
c = reference length
F = complex potential $\phi + i\psi$
FR = potential
H = simplified gust function ($=\phi(k)e^{-ik}$)
I,J = unit vectors parallel and perpendicular to the average uniform motion of the bodies
i,j = imaginary units for space and time, respectively
k = $\omega/2$
q = magnitude of the velocity tangential to the body surface normalized by U_∞
r = radius vector from origin of moving axis to point fixed in moving frame of reference normalized by c
t = nondimensional time (= time U_∞/c)
U_g = nondimensional amplitude of gust
U_T = nondimensional speed at which gust appears to advance relative to a coordinate system moving with speed U_∞ in negative direction
U_∞ = average speed at which the bodies are moving in the negative X direction
V_c = nondimensional speed of fluid as viewed in moving coordinate system
$\mathbf{V}_f$ = nondimensional velocity of moving coordinate system
$\mathbf{V}_g$ = nondimensional velocity of gust onset flow
V_p = nondimensional speed of a fluid particle in the wake
$\mathbf{V}_r$ = nondimensional velocity of a point fixed in the moving coordinate system
w = nondimensional magnitude of the velocity normal to the body surface
X,Y = coordinates oriented parallel and perpendicular to the direction of average motion (nondimensional)
x,y = body coordinates (nondimensional)
z = $x + iy$
α = angular orientation of a wake element
Γ = circulation (nondimensional)
γ = wake vorticity (nondimensional)
Δc = short segment of wake fluid particles
Δq = tangential velocity difference at the body trailing edge
δ = small linear or angular displacement (normalized)
$\Delta\tau$ = short segment of wake
ζ = coordinate of source or vortex point
η = amplitude of wave height for water wave gust
λ = angular orientation of a body source element
σ = body element source strength (nondimensional)
τ = nondimensional distance along the wake
Φ = total normalized potential as viewed in the body fixed coordinate system less the potential of the uniform flow moving with speed U_∞
ϕ = component normalized potential
$\phi(k)$ = Sears gust function
Ω = angular velocity of a body
ω = reduced frequency (= frequency c/U_∞)

Subscripts and Superscripts

d = disturbance flow
e = equivalent velocity
g = gust flow
l = receiving element midpoint index
m = sending element index
n = wake element index
o = onset flow
Q = quasi steady flow
r,s,t = body identification indices
s_x,s_y = component of steady onset flow in x and y directions
w = wake flow
x,y = components in the x and y directions, respectively
θ = component in the angular direction (positive counterclockwise)
$1,2$ = first and second source element end points

Introduction

THE theory for two-dimensional flow about thin plates in oscillatory motion developed by various authors (see Fung[1] for a historical survey), has been extended to include the effects of thickness by Woods,[2] Kussner,[3] Hewson-Browne,[4] and Van De Vooren and Van De Vel.[5] Woods, Kussner, and Hewson-Browne were primarily interested in obtaining forces and moments; consequently, they made no provisions to determine the surface pressures. It was noted by Van De Vooren and Van De Vel that viscous effects on lift forces and moment are larger than the effects of thickness. These authors therefore undertook to determine the unsteady pressure distribution as a critical first step in the determination of viscous effects.

In all of the thick-airfoil investigations mentioned, calculated results were presented only for symmetrical bodies at zero mean incidence whose circle-airfoil transformation was known and relatively simple.

The method described herein extends the oscillatory theory on several fronts; 1) a body of arbitrary shape is accommodated with ease, 2) bodies performing small oscillations about any equilibrium position are considered, and 3) the present method uses a potential-flow procedure that does not require transformation methods and, therefore, allows for more than

Received January 15, 1970; revision received May 20, 1970. This research was carried out under the Naval Ship Systems Command Hydrofoil Exploratory Development Program SF-013-02-01 administered by the Naval Ship Research and Development Center prepared under the Office of Naval Research.

* Senior Engineer, Structural Mechanics Section. Associate Fellow AIAA.

one body. As a result, the aerodynamic interference of several bodies vibrating independently may be determined, whether or not they possess circulation.

Other methods have been developed for the step-by-step solution of nonlinear unsteady potential-flow problems for a single body,[6] for two bodies,[7] and for a single three-dimensional wing.[8] Although these methods can be used to solve problems of small-amplitude motion, they were not developed for that purpose and are not well suited to it. Lacking any other basis, comparisons with the present method are given in Figs. 4–6. The nonlinear methods use the transient approach to solve all problems; as a consequence, the calculations must range over long time periods if purely periodic motions are desired. Also, if the amplitudes are small enough, the large computational effort required for the nonlinear method is wasted because nonlinearities will not exist. Additionally, the the results may not be very accurate. The flow properties are not separated into steady and unsteady parts, therefore, for small-amplitude motion, the unsteady part is obtained as the difference between two values (total minus steady) that are almost identical. A linearized method then, such as the one presented herein, has a definite place in the theory of simple-harmonic motions.

Description of the Problem

It is desired to find the unsteady flow about one or more lifting two-dimensional bodies of arbitrary shape oscillating about their equilibrium positions. It will be assumed that the amplitude of motion is small and that the two-dimensional, incompressible potential-flow model applies. Since an arbitrary periodic motion can be built up of its Fourier components, attention will be focused on the solution for those components. The motion will then be simple-harmonic and the resulting flow a function of the frequency of oscillation.

The governing equations of unsteady potential-flow are the Laplace equation

$$\nabla^2\Phi = 0 \tag{1}$$

and the Bernoulli equation

$$C_p = (V_r^2 - V_c^2) - 2\dot{\Phi} \tag{2}$$

where the Bernoulli equation is written with reference to a moving coordinate system fixed in the body being considered (see Milne-Thompson[9] p. 87). The vector $\mathbf{V}_c$ is the normalized† fluid velocity as viewed in this coordinate system, and the vector $\mathbf{V}_r$ is the velocity of a point fixed in the same system, i.e., $\mathbf{V}_r = \mathbf{V}_f + \mathbf{r} \times \boldsymbol{\Omega}$, ($V_c^2 = \mathbf{V}_c \cdot \mathbf{V}_c$ and $V_r^2 = \mathbf{V}_r \cdot \mathbf{V}_r$). In addition to these equations, a vorticity-conservation condition must be applied. Specifically, any loss of circulation of a body must show up in the wake of that body as shed vorticity so that the total vorticity of the system remains constant. The shed vortices flow off the body at the trailing edge and down the trailing streamline with the speed of the surrounding fluid. It is assumed that the location of the trailing streamline and the velocity along it are given, to first order, by their steady values.

The solution of the steady Neumann problem for lifting bodies of arbitrary shape and number is given in Ref. 10. The basic idea of the present paper is to reduce the unsteady problem with moving boundaries to an equivalent problem with fixed boundaries that is accurate through $0(\delta)$,‡ where δ is the amplitude of motion, so that the methods of Ref. 10 can be applied.

† All velocities are normalized by the average forward speed of the bodies (U_∞). All lengths are normalized by a reference chord length c. All other quantities are normalized by a combination of U_∞ and c.

‡ A function f is of $0(\delta)$ if $\lim_{\delta \to 0} \left|\frac{f}{\delta}\right| < \infty$.

Steady Potential Flow

The numerical solution of the steady Neumann boundary-value problem as given in Ref. 10 is reviewed here. The potential or velocity anywhere in the fluid can be found once the velocity distribution normal to all boundaries is known. The solution is effected by breaking up the potential (Φ) and velocity (q and w) into the onset (o) and disturbance (d) components.

$$\Phi = \phi_o + \phi_d \quad \text{potential} \tag{3a}$$

$$q = q_o + q_d \quad \text{tangential velocity} \tag{3b}$$

$$w = w_o + w_d \quad \text{normal velocity} \tag{3c}$$

The onset flow is the flow that would exist if the body were not present, and the disturbance flow exists to deflect the onset flow in such a way that no fluid passes through the body ($w = 0$). The disturbance flow is generated by a distribution of singularities on the surfaces of the source type. In particular, the surfaces of the bodies are approximated by a large number of connecting straight-line elements. Each element possesses a constant source strength σ but the strength varies from element to element. The complex velocity at the midpoint of element l due to the source element m (of unit strength) is A_{lm}

$$A_{lm} = q_{lm} - iw_{lm} = e^{i\lambda} dF_{lm}/dZ \tag{4}$$

where

$$dF_{lm}/dZ = e^{-i\lambda_m} \ln(Z_l - \zeta_{1m}/Z_l - \zeta_{2m}) \tag{5}$$

Here Z is the complex coordinate of the receiving point, ζ_1 and ζ_2 are the complex coordinates of the end points of the sending element, and λ is the angular orientation of an element. The source distribution (σ_m) is adjusted until the normal disturbance velocity (w_d) is equal but opposite to the onset normal velocity (w_o), represented by

$$w_{o_l} = -AI_{lm}\sigma_m\S$$

or

$$\sigma_m = -AI_{lm}^{-1} w_{o_l} \tag{6}$$

where AI_{lm} is the imaginary part of A_{lm}. Once the source distribution (σ_m) is known, the disturbance flow anywhere in the field can easily be found. Specifically, the tangential velocity distribution (q_l) is

$$q_{d_l} = AR_{lm}\sigma_m \tag{7}$$

where AR_{lm} is the real part of A_{lm}. Also, the potential distribution is

$$\phi_{d_l} = FR_{lm}\sigma_m \tag{8}$$

where FR_{lm} is the real part of F_{lm} defined implicitly in Eq. (5). The total solution for the tangential velocity and the potential is obtained from Eqs. (3a) and (3b).

Solution

Reduction of the Unsteady Flow

The unsteady boundary-value problem involving moving boundaries is to be reduced to an unsteady problem involving stationary boundaries. Fixing the boundaries for a single body is easily accomplished by simply adopting body-fixed coordinates. This is not true for more than one body since, generally, there will be relative motion among the bodies. Since the motions are assumed small (characterized by the

§ The usual summation convention is used here and henceforth. For example, $w_{ol} = -AI_{lm}\sigma_m$ means that $w_{o_l} = -\sum_{m=1}^{n} AI_{lm}\sigma_m$.

amplitudes δ^s ($s = 1, 2, \ldots$), where $\delta^s \ll 1$ and s refers to a particular body), an expansion in the amplitude about the steady position can be effected.

Assume that there is fixed in each body a coordinate system that is used to describe the flow about that body. When dealing with interference, the coordinate system of the body affected is used to describe that interference. An expansion about the body equilibrium positions can be made by using the δ^s ($s = 1, 2, \ldots$) as the expansion parameters. Combining Eqs. (6) and (7) gives

$$-q_d = ARAI^{-1}w_o \P \tag{9}$$

Expanding Eq. (9) about $\delta^s = 0$ gives

$$-q_d = ARAI^{-1}w_o + \sum_{s=1} \delta^s (\partial ARAI^{-1}w_o/\partial\delta^s) + \ldots \tag{10}$$

Here, AR, AI^{-1} and their derivatives are evaluated at the steady equilibrium position; that is, at $\delta^s = 0$, and subscripts are dropped for convenience. Since the boundary values w_o are determined in the body-fixed coordinate systems, they are not functions of δ^s. Evaluation of the derivatives proceeds as follows:

$$\partial ARAI^{-1}/\partial\delta^s = (\partial AR/\partial\delta^s)AI^{-1} + AR\partial AI^{-1}/\partial\delta^s \tag{11}$$

Since

$$\partial(AI^{-1}AI)/\partial\delta^s = 0$$

it follows that

$$\partial AI^{-1}/\partial\delta^s = -AI^{-1}(\partial AI/\partial\delta^s)AI^{-1}$$

or Eq. (11) may be written as

$$\partial ARAI^{-1}/\partial\delta^s = (\partial AR/\partial\delta^s)AI^{-1} + ARAI^{-1}(\partial AI/\partial\delta^s)AI^{-1} \tag{12}$$

Combining Eqs. (10) and (12) gives

$$-q_d = ARAI^{-1}\left(w_o - \sum_{s=1} \delta^s \frac{\partial AI}{\partial\delta^s} AI^{-1}w_o\right) + \sum_{s=1} \delta^s \frac{\partial AR}{\partial\delta^s} AI^{-1}w_o \tag{13}$$

The matrix AI and its derivative $\partial AI/\partial\delta^s$ can be partitioned to illustrate the effects of the bodies on each other, as follows:

$$AI = \begin{bmatrix} AI^{(11)} & AI^{(12)} \ldots & AI^{(1s)} \ldots \\ AI^{(21)} & AI^{(22)} \ldots & AI^{(2s)} \ldots \\ \cdot & & \\ \cdot & & \\ \cdot & & \\ AI^{(r1)} & AI^{(r2)} \ldots & AI^{(rs)} \ldots \end{bmatrix} \tag{14}$$

The submatrix of influence coefficients $AI^{(rs)}$ indicates that body s is affecting body r. Since interference effects are determined in the coordinate system of the body receiving the influence, the r coordinate system is used in calculating $AI^{(rs)}$. The only portions of AI affected by changing δ^s are those that are associated with body s. Therefore

$$\partial AI^{rt}/\partial\delta^s = 0 \text{ when } r \neq s \text{ and when } t \neq s \tag{15}$$

Also, the effect of body s on itself does not change with δ^s since body-fixed coordinates are used and the body is assumed to be rigid.

$$\partial A^{rt}/\partial\delta^s = 0 \text{ when } [r = s \text{ and when } t = s] \tag{16}$$

¶ The terms with double subscripts are elements of matrices. When the subscripts are dropped it is understood that the matrix itself is being considered. Thus, the elements of the matrix AR are AR_{lm} and the elements of q_d are q_{d_l}.

When $t = s$, the derivative refers to the effect of the vibrating body on the body to which the observer is fixed, that is, body r. When $r = s$, the derivative refers to the effect of body t as it appears to vibrate, on body s. When the observer is fixed to the body that is vibrating, the rest of the bodies—in particular, body t appear to be vibrating with amplitude $-\delta^s$.

If Eqs. (15) and (16) are considered, the derivative $\partial AI/\partial\delta^s$ may be written in partitioned matrix form as follows:

$$\partial AI/\partial\delta^s = AI_\delta = \begin{bmatrix} 0 & 0 & \ldots & 0 & A_\delta{}^{1s} & 0 & \ldots \\ 0 & 0 & \ldots & 0 & A_\delta{}^{2s} & 0 & \ldots \\ \cdot & & & & & & \\ \cdot & & & & & & \\ \cdot & & & & & & \\ 0 & 0 & & 0 & A_\delta{}^{s-1,s} & 0 & \ldots \\ A_\delta{}^{s1} & A_\delta{}^{s2} & \ldots & A_\delta{}^{ss-1} & 0 & A_\delta{}^{ss+1} & \ldots \\ 0 & 0 & \ldots & 0 & A_\delta{}^{s+1,s} & 0 & \ldots \end{bmatrix} \tag{17}$$

A similar matrix may be written for $\partial AR/\partial\delta^s$. The derivative of $A^{rs}(=AR^{rs} + iAI^{rs})$ with respect to δ^s may be obtained from Eqs. (4) and (5)

$$\frac{\partial A^{rs}}{\partial\delta^s} = \frac{\partial}{\partial\delta^s}\left[e^{i(\lambda^r - \lambda^s)}\ln\left(\frac{Z^r - \zeta_1{}^s}{Z^r - \zeta_2{}^s}\right)\right] = \frac{-i\partial\lambda^s}{\partial\delta^s} A^{rs} + e^{i(\lambda^r - \lambda^s)}\left[\frac{-\partial\zeta_1{}^s/\partial\delta^s}{Z^r - \zeta_1{}^s} + \frac{\partial\zeta_2{}^s/\partial\delta^s}{Z^r - \zeta_2{}^s}\right] \tag{18}$$

$$\frac{\partial A^{st}}{\partial\delta^s} = i\frac{\partial\lambda^s}{\partial\delta^s} A^{st} + e^{i(\lambda^s - \lambda^t)}\left[\frac{\partial Z/\partial\delta^s}{Z^s - \zeta_1{}^t} - \frac{\partial Z^s/\partial\delta^s}{Z^s - \zeta_2{}^t}\right] \tag{19}$$

The boundary-value problem with moving boundaries, for one or more bodies, has been reduced to an equivalent boundary-value problem with boundaries fixed at their steady equilibrium positions. The solution is given by Eq. (13) as

$$q_d = ARAI^{-1}w_{o_e} + q_{o_e} \tag{20}$$

where w_{o_e} is the equivalent normal boundary-value distribution given in matrix form by

$$\{w_{o_e}\} = \left[I - \sum_{s=1} \delta^s(\partial AI/\partial\delta^s)AI^{-1}\right]\{w_o\} \tag{21}$$

where I is the identity matrix. In Eq. (20), q_{o_e} is an additional tangential onset flow that must be added.

$$\{q_{o_e}\} = \left[\sum_{s=1} \delta^s(\partial AR/\partial\delta^s)AI^{-1}\right]\{w_o\} \tag{22}$$

An expression similar to Eq. (20) can be written for the disturbance potential

$$\phi_d = FRAI^{-1}w_{o_e} + \phi_{o_e} \tag{23}$$

where, in matrix notation,

$$\{\phi_{o_e}\} = \left[\sum_{s=1} \delta^s(\partial FR/\partial\delta^s)AI^{-1}\right]\{w_o\} \tag{24}$$

$$\frac{\partial F^{rs}}{\partial\delta^s} = -iF^{rs} + e^{-i\lambda^s}\{ln(Z^r - \zeta_1{}^s)d\zeta_1{}^s/d\delta^s - ln(Z^r - \zeta_2{}^s)d\zeta_2{}^s/d\delta^s\} \tag{25}$$

and

$$\partial F^{st}/\partial\delta^s = e^{-i\lambda^t} ln(Z^s - \zeta_1{}^2/Z^s - \zeta_2{}^t)dZ^s/d\delta^s \tag{26}$$

The onset flow (w_o and q_o) may be split up into steady terms (w_{s_o} and q_{s_o}) which are of 0(1) and unsteady terms ($\bar{w}_\delta e^{j\omega t}$ and $\bar{q}_\delta e^{j\omega t}$ which are of $0(\delta)$.

$$w_o = w_{s_o} + \bar{w}_\delta e^{j\omega t}$$
$$q_o = q_{s_o} + \bar{q}_\delta e^{j\omega t} \tag{27}$$

The expressions for w_{o_e} and q_{o_e} then become

$$w_{o_e} = w_{s_o} \qquad 0(1)$$

$$+ \left\{\bar{w}_\delta - \left(\sum_{s=1} \bar{\delta}^s(\partial AI/\partial\delta^s)AI^{-1}\right)w_{s_o}\right\}e^{j\omega t} \qquad 0(\delta) \quad (28)$$

$$q_{o_e} = 0 \qquad 0(1)$$

$$+ \left(\sum_{s=1} \bar{\delta}^s(\partial AR/\partial\delta^s)AI^{-1}\right) w_{s_o}e^{j\omega t} \qquad 0(\delta) \quad (29)$$

where $\delta = \bar{\delta}e^{j\omega t}$ and terms of $0(\delta^s)$ and higher have been dropped. The 0(1) solution for q_d is then obtained by placing the 0(1) term of w_{o_e} and q_{o_e} in Eq. (20); likewise, the $0(\delta)$ term is obtained by using the term of $O(\delta)$ for w_{o_e} and q_{o_e} in Eq. (20). The same procedure holds true for ϕ_d in Eq. (23).

Quasi-Steady Flow

The unsteady disturbance flow consists of a vorticity-free flow and a flow that possesses circulation and vorticity. The former is the quasi-steady flow while the latter is the circulation and wake flow. The quasi-steady flow, which is being considered here, satisfies all of the boundary conditions except the Kutta condition. To obtain this flow (or flows), all that is required is the specification of the normal boundary values w_o and the body motions, δ^s in Eqs. (20) and (23). The onset flow is caused by a steady velocity ($U_\infty\mathbf{I}$) of 0(1), an unsteady velocity generated by a gust ($\mathbf{V}_g$) of $0(\delta)$ and an unsteady velocity caused by body motions ($\mathbf{V}_\delta$) of $0(\delta)$. Then

$$w_o = (\mathbf{I} + \mathbf{V}_g + \mathbf{V}_\delta)\cdot\mathbf{n} = w_{s_o} + \bar{w}_{Q_o}e^{j\omega t} \quad (30a)$$

$$q_o = (\mathbf{I} + \mathbf{V}_g + \mathbf{V}_\delta)\cdot\mathbf{t} = q_{s_o} + \bar{q}_{Q_o}e^{j\omega t} \quad (30b)$$

where the subscript Q has replaced the subscript δ in Eq. (27) to indicate quasi-steady flow. The body motions are simple-harmonic in the body-fixed directions x, y, and θ. For small motions, $\mathbf{V}_\delta$ can be written as

$$\mathbf{V}_\delta = -[\mathbf{i}\delta_x + \mathbf{j}\delta_y - \mathbf{i}(y - y_R)\delta_\theta + \mathbf{j}(x - x_R)\delta_\theta]j\omega e^{j\omega t} + [-\mathbf{i}V_{s_y} + \mathbf{j}V_{s_x}]\delta_\theta e^{j\omega t} \quad (31)$$

Here j is the time imaginary unit, and $\mathbf{i}$ and $\mathbf{j}$ are the unit vectors in the x and y directions, respectively. Also, $\mathbf{V}_{s_x} = \mathbf{I}\cdot\mathbf{i}$ and $\mathbf{V}_{s_y} = \mathbf{I}\cdot\mathbf{j}$.

Two types of gust flows are considered: the classical gust, where only a vertical velocity exists, and a gust field generated by traveling water waves. Specifically, the classical gust is specified by

$$\mathbf{V}_g = \mathbf{J}U_g e^{-jX\omega/U_T}e^{j\omega t}$$
$$\phi_{o_g} = 0 \quad (32)$$

and the water-wave gust field by

$$\mathbf{V}_g = \mathbf{I}(u - jv) + \mathbf{J}(v + ju)$$

$$u - jv = \eta[j(1 - U_T/U_T)\omega e^{\omega Y/U_T}]e^{-jX\omega/U_T}e^{j\omega t} \quad (33a)$$

$$\phi_{o_g} = Re\eta[-(1 - U_T)e^{\omega Y/U_T}]e^{jX\omega/U_T}e^{j\omega t} \quad (33b)$$

where $\mathbf{I}$ and $\mathbf{J}$ are parallel and perpendicular, respectively, to the direction in which the gust is traveling. Also, X and Y are the coordinates associated with $\mathbf{I}$ and $\mathbf{J}$. The term U_T is the speed of travel of the gust relative to the body and U_g is the amplitude [$0(\delta)$] of the classical gust and η is the amplitude of the wave at the surface. The expression given in Eq. (33b) is obtained from Eq. (2) on p. 394 of Milne-Thompson.[9] Specifically, a Galilean transformation is applied whereby the coordinate system is changed from one fixed in the water to one moving with constant velocity U_∞ in the negative X direction. It should be noted that the current theory does not take into account free surface effects. The water wave is used only as gust flow of interest.

The terms w_{s_o} and w_{Q_o} for the quasi-steady flow are complete except for the determination of the derivatives $\partial\lambda/\partial\delta$, $\partial\zeta_1/\partial\delta$, $\partial\zeta_2/\partial\delta$, and $\partial Z/\partial\delta$. The vibratory motion of the body can be expressed as

$$\delta = (\bar{\delta}_x + \bar{\delta}_y + \bar{\delta}_\theta)e^{j\omega t} \quad (34)$$

Therefore

$$\partial\lambda/\partial\delta = \partial\lambda/\partial\delta_\theta = 1 \quad (35)$$

and

$$\delta\frac{\partial Z}{\partial\delta} = (\bar{\delta}_x\partial Z/\partial\delta_x + \delta_y\,\partial Z/\partial\delta_y + \delta_\theta\,\partial Z/\partial\delta_\theta)e^{j\omega t} \quad (36)$$

where

$$\partial Z/\partial\delta_x = 1 \quad \partial Z/\partial\delta_y = i \quad \partial Z/\partial\delta_\theta = i(Z - ZR) \quad (37)$$

Expressions similar to Eq. (37) may be written for $\partial\zeta_1/\partial\delta$ and $\partial\zeta_2/\partial\delta$.

Placing the terms w_{s_o} and w_{Q_o} into Eqs. (28) and (29), and the terms w_{o_e} and q_{o_e} into Eqs. (20) and (23) gives the quasi-steady solution for both 0(1) and $0(\delta)$. The steady term of 0(1) is q_s, and the unsteady term of $0(\delta)$ is q_Q

$$q_s = q_{s_o} + q_{s_d} \quad (38a)$$

$$q_Q = q_{Q_o} + q_{Q_d} \quad (38b)$$

Circulatory and Wake Flow

The quasi-steady solution satisfies the surface boundary conditions (i.e., that the fluid normal velocity at the surface be equal to the surface normal velocity) but does not satisfy the Kutta condition. To satisfy the Kutta condition, a circulatory flow is introduced about each lifting body.** The circulation possesses a steady part of 0(1) and an unsteady part of $0(\delta)$. Because vorticity is conserved, the unsteady circulation must be accompanied by a vortex wake. The loss in circulation (Γ) must appear as shed vorticity (γ) at the trailing edge (or separation point) of each lifting body. Specifically,

$$(\gamma V_p)_{T.E.} = -d\Gamma/dt = -j\omega\bar{\Gamma}e^{j\omega t} \quad (39)$$

where V_p is the velocity at which the vorticity is carried away, and $\bar{\Gamma}$ is the time-complex amplitude of the circulation.

The vortices generated at the trailing edge during a unit of time are swept down the trailing streamline of the body. The total strength of the vorticity remains unchanged as the vortices travel down the streamline even though the vorticity strength per unit length may change because of dilation. If $\gamma\Delta c$ is the strength of this segment of vorticity, where Δc is a short segment of the vortex wake attached to fluid particles, then

$$D(\gamma\Delta c)/dt|_{\text{particle}} = 0 \quad (40)$$

It can be shown by Ref. 11 that if $\gamma = f(\tau)e^{j\omega t}$, Eq. (40) leads to

$$\gamma(t,\tau) = [(\gamma V_p)_{T.E.}/V_p(\tau)e^{-j\omega T(\tau)} \quad (41)$$

where

$$T(\tau) = \int_0^\tau \frac{d\lambda}{V_p(\lambda)} \quad (42)$$

And τ is distance measured along the wake.

** More accurately, a circulatory flow is introduced about each body that can maintain a circulation, that is, one that requires a Kutta condition.

Combining Eqs. (39) and (41) gives

$$\gamma(t,\tau) = \bar{\Gamma}[(-j\omega/V_p(\tau))e^{-j\omega T(\tau)}]e^{j\omega t} \tag{43}$$

This equation gives the vorticity distribution in the wake of a particular body in terms of the circulation of that body and in terms of the steady velocity distribution $[V_p(\tau)]$ along the stagnation streamline. Eq. (43) holds true for each body. Considering Eq. (43), the onset potential field generated by the vortex wake of a particular body can be written as

$$\bar{\Gamma}e^{j\omega t}(-j\omega)ReG \tag{44}$$

where

$$G = \frac{i}{2\pi}\int_0^\infty \frac{e^{-j\omega T}}{V_p} ln(Z - \zeta_w)d\tau$$

Here, Z is the complex coordinate of a point on a body and ζ_w is the complex coordinate of a point in a wake. The term G may be integrated by parts as follows,††

$$G = (1/j\omega)i/2\pi[\ln(Z - \zeta_{w_o}) + I_1] \tag{45}$$

where

$$I_1 = \int_0^\infty \frac{e^{-i\omega T}}{Z - \zeta_w} d\zeta$$

and where ζ_{w_o} denoted $\zeta_w(\tau = 0)$ that is, the body trailing edge.

In order to generate an onset circulatory flowfield, a point vortex is placed within each body at the trailing edge. The potential field due to a point vortex is

$$\bar{\Gamma}e^{j\omega t}\ln(Z - \zeta_{w_o}) \tag{46}$$

Adding Eqs. (44) and (46) note [Eq. (45)] gives

$$\phi_{w_o} = \bar{\Gamma}\bar{\phi}_{w_o}$$

where

$$\bar{\phi}_{w_o} = e^{j\omega t}(-I_1)$$

The tangential and normal onset velocities‡‡ are given by

$$q_{w_o} - iw_{w_o} = \bar{\Gamma}(\bar{q}_{w_o} - i\bar{w}_{w_o}) \tag{47}$$

where

$$\bar{g}_{w_o} - i\bar{w}_{w_o} = e^{j\omega t}e^{i\lambda}\{-i\omega I_2 + 1/(Z - \zeta_{w_o})\}$$

and where

$$I_2 = \int_0^\infty \frac{e^{-i\omega T}d\tau}{V_p(Z - \zeta_w)}$$

Introducing Eq. (47) into Eq. (21) and retaining only terms of $O(\delta)$ gives

$$w_{oe} = \bar{\Gamma}\bar{w}_{w_o}, \quad q_{oe} = 0 \tag{48}$$

Placing these boundary values into Eq. (20) gives the disturbance tangential velocity,

$$q_{w_d} = \bar{\Gamma}\bar{g}_{w_d} \tag{49}$$

where $\bar{q}_{w_d}$ is obtained from Eq. (20) by using $\bar{w}_{w_o}$. The total tangential velocity for one circulation and wake is the sum of the disturbance velocity and the onset velocity. The total tangential velocity for all of the circulations and wakes is obtained by summing the contributions of all the bodies.

$$q_w = \sum_{s=1} \bar{\Gamma}^s(\bar{q}_{w_d}{}^s + \bar{q}_{w_o}{}^s) \tag{50}$$

Likewise, for the potential

$$\phi_w = \sum_{s=1} \bar{\Gamma}^s(\bar{\phi}_{w_d} + \bar{\phi}_{w_o}) \tag{51}$$

The solution for the circulation and wake flow is now complete except for the determination of the circulation (Γ) in each body and the evaluation up the integrals I_1 and I_2.

Evaluation of I_1 and I_2

The approximate evaluation of I_1 and I_2 for a particular vortex wake can be effected by breaking up each wake as depicted in Fig. 1.

It is assumed that $V_p(\tau)$ is constant over each straight-line element but that V_p varies from element to element. In this case

$$T(\tau) = T_n + \tau e_n{}^{ia} \tag{52}$$

where

$$-\Delta\tau_n/2 \leqslant \tau \leqslant \Delta\tau_n/2$$

and where

$$T_n = \sum_{\lambda=1}^{n-1} \Delta\tau_\lambda/V_{p\lambda}$$

The integrals I_1 and I_2 are then approximated by

$$I_1 = \sum_{n=1} e^{-j\omega T_n}e^{ia_n}\int_{-\Delta\tau_n/2}^{\Delta\tau_n/2} \frac{e^{-j\omega\tau/V_p}}{Z - \zeta_{w_n} - \tau e^{ia_n}}\, d\tau$$

$$I_2 = \sum_{n=1} e^{-\omega T_n}\frac{1}{V_{p_n}}\int_{-\Delta\tau_n/2}^{\Delta\tau_n/2} \frac{e^{-j\omega\tau/V_{pn}}}{Z - \zeta_{w_n} - \tau e^{ia_n}}\, d\tau$$

where $d\zeta = d\tau e^{ia}$ over an element. The subintegral common to both of these is

$$I_n = \int_{-\Delta\tau_n/2}^{\Delta\tau/2} \frac{e^{-j\omega\tau V_{pn}}}{Z - \zeta_{w_n} - \tau e^{ia_n}} = \int_{-C_n}^{C_n} \frac{e^{-ju}}{P_n - u}\, du$$

where

$$C_n = \Delta\tau_{nw}/2V_{p_n}\ P_n = \omega(Z - \zeta_{w_n})/V_{p_n}e^{i\alpha_n},\quad u = \omega\tau/V_{pn}$$

It can be shown by Ref. 11, pp. 26–30, that $\mathbf{I}_n$ is expressible in terms of the exponential integral as follows:

$$I = \tfrac{1}{2}([A + B] + j[i(A - B)]) \tag{53}$$

where

$$A = -e^{iP}\{E_1[i(P + C)] - E_1[i(P - C)] + 2\pi i\delta_A\}$$

$$B = -e^{-iP}\{E_1[-i(P + C)] - E_1[-i(P - C) - 2\pi i\delta_B\}$$

$$\delta_A = \begin{cases} 1 & |ReP| < C \text{ and } Re(iP) < 0 \\ 0 & \text{otherwise} \end{cases}$$

$$\delta_B = \begin{cases} 1 & |ReP| < C \text{ and } Re(-iP) < 0 \\ 0 & \text{otherwise} \end{cases}$$

Circulation

The unsteady Kutta condition is given in Ref. 12 as: *The difference in tangential velocity between the upper and lower surfaces at the trailing edge is equal to the strength of the shedding vorticity.*

If Δq represents this difference, then

$$\Delta q = \Delta q_Q + \sum_{s=1} \Gamma^s(\Delta q_{w_o}{}^s + \Delta q_{w_d}{}^s) = \gamma(\tau = 0) \tag{54}$$

†† Note that from Eq. (42) $dT = d\tau/V_p$. The term $\ln(z - \infty)$ is a constant and, therefore, can be ignored.

‡‡ The onset flow $\ln(z - \zeta_{w_o})$ is generated by a point vortex located at the body trailing edge. The corresponding disturbance flow must be obtained by indirect means because of the failure, in the face of such strong singularity, of the methods considered here and in the method of Giesing.[10] The details are given by Giesing[11] but, in general, the method of attack is to obtain a full (onset plus disturbance) solution for the unique circulatory flow and subtract the onset flow, which is due to the trailing-edge vortex. This gives the desired disturbance flow.

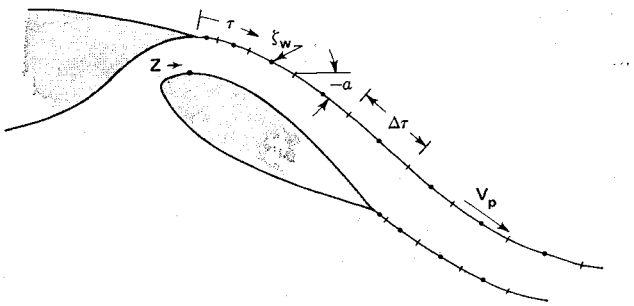

Fig. 1 Schematic of airfoils and vortex wakes.

Eq. (54) is made to hold at each trailing edge, thus furnishing as many equations as there are unknown values of circulation $\bar{\Gamma}^s$. From Eq. (39),

$$\gamma_{T.E.} = \gamma(\tau = 0) = -j\omega\bar{\Gamma}e^{j\omega t}/V_p{}^s(\tau = 0) = -\bar{\Gamma}A^s \quad (55)$$

Introducing the notation

$$D^s = \Delta q_{w_o}{}^s + \Delta q_{w_d}{}^s + A^s$$

and adding the superscript r to indicate the trailing edge at which Eq. (54) is made to apply, gives

$$\sum_{s=1} \bar{\Gamma}^s D^{rs} = \Delta q_Q{}^r \quad (56)$$

which can be easily solved for the values of $\bar{\Gamma}^s$.

The solution for the circulation and wake flow is now complete.

Pressure, Forces and Moments

The unsteady Bernoulli equation for a coordinate system fixed in a moving body is given by Eq. (2) and Ref. 11, p. 37 as

$$C_p = C_{p_1} + C_{p_2} = (p - p_\infty)/\tfrac{1}{2}\rho U_\infty{}^2 \quad (57a)$$

$$C_{p_1} = (V_r{}^2 - q^2) \quad (57b)$$

$$C_{p_2} = -2\dot{\phi} \quad (57c)$$

where $\mathbf{V}_r$ is the velocity of a fixed point in the body-fixed frame of reference.

$$\mathbf{V}_r = -I + \mathbf{V}_\delta \quad (58)$$

where $\mathbf{I}$ is the steady velocity of 0(1) and $\mathbf{V}_\delta$, as defined in Eq. (31), is the velocity due to vibration of $0(\delta)$. The tangential velocity q is the sum of the steady velocity q_s of 0(1) and the unsteady velocity q_δ of $0(\delta)$. The unsteady tangential velocity q_δ is the sum of the quasi-steady velocity q_Q and the wake velocity q_w. Retaining terms of 0(1) and $0(\delta)$ for q^2 gives

$$q^2 = q_s{}^2 + 2q_s(q_Q + q_w) + \ldots \quad (59)$$

Retaining terms of 0(1) and $0(\delta)$ for $V_r{}^2$ gives

$$V_r{}^2 = \mathbf{V}_r \cdot \mathbf{V}_r = 1 - 2\mathbf{V}_s \cdot \mathbf{V}_\delta + \ldots$$

The term $\dot{\phi}$ is just $j\omega\phi$, where

$$\phi = \phi_Q + \phi_w$$

The pressure equation is then

$$C_p = 1 - q_s{}^2 \quad 0(1)$$

$$-2[q_s(q_Q + q_w) + j\omega\phi + \mathbf{I} \cdot \mathbf{V}_\delta] \quad 0(\delta) \quad (60)$$

Eq. (60) holds for each body. If the pressure on a stationary body in the presence of a moving body is desired, $\mathbf{V}_\delta$ in Eq. (60) is zero. The forces and moments on each body are obtained by direct integration of the pressures over the surfaces.

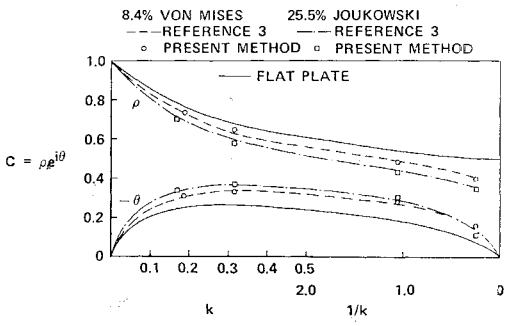

Fig. 2 Comparison of the Theodorsen function for airfoils of various thickness.

Calculated Results

All the equations described so far have been programed in FORTRAN IV for both one body and two bodies. In addition, a method for calculating the location of trailing streamlines and the velocity distribution along them has been developed (see Ref. 11).

Single-Body Configuration Cases

Kussner[3] has developed a theory for a single symmetric body whose circle-airfoil transformation is known. This theory deals with forces and moments only. Fig. 2 shows a comparison of the present method with Kussner's results for two symmetric airfoils: one 8.4-percent thick, the other 25.5-percent thick. The Theodorsen function (circulatory part of the lift) is shown as a function of the reduced frequency $k = \omega/2$. For reference, the results for a flat plate are also given. Kussner's results and those of the present method are in good agreement.

Van De Vooren and Van De Vel[5] have developed a theory for a single airfoil that gives the surface pressure distribution. Again, the circle-airfoil transformation must be known. The airfoil shown in Fig. 3 is generated by using the parameter θ of

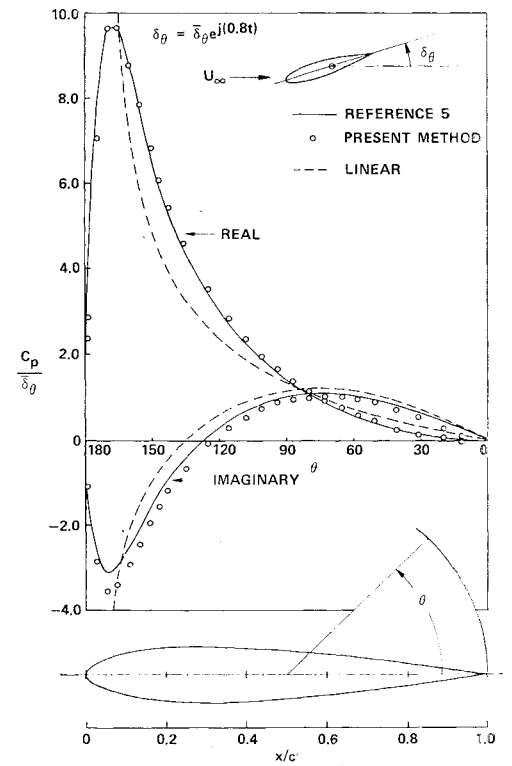

Fig. 3 Comparison of the pressure distributions as calculated by the present method and the method of Ref. 5 for a 13% thick airfoil.

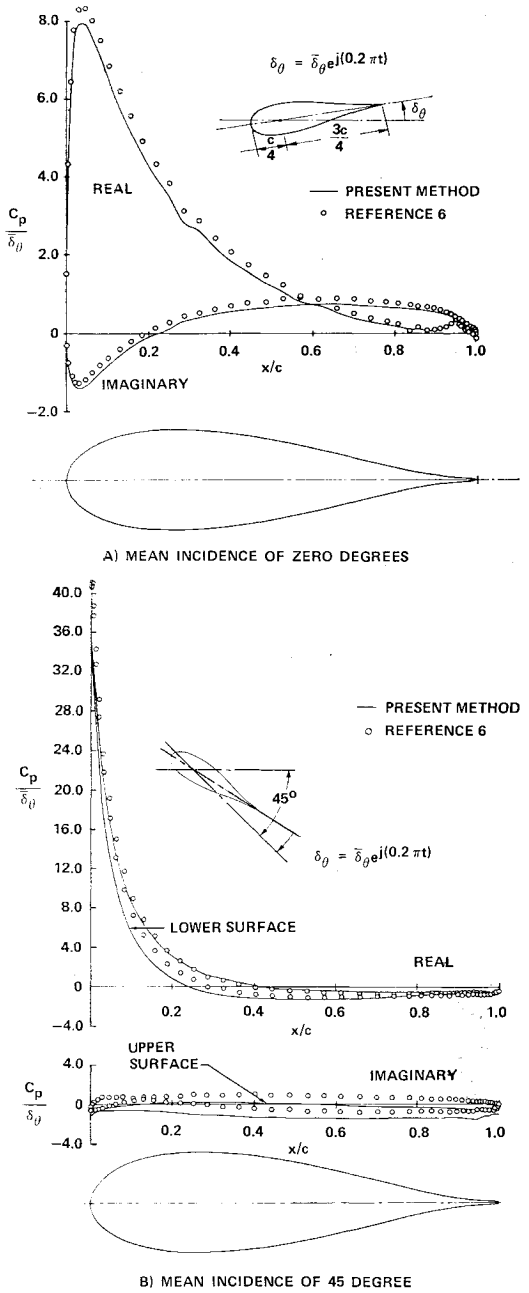

Fig. 4 Comparison of the pressure distributions as calculated by the present method and the method of Ref. 6 for a 25.5% thick Joukowski airfoil.

Ref. 5, Eq. (4.1) where $x = \frac{1}{2}(1 + \cos\theta)$. The pressure distribution is plotted vs θ in the figure. Only the upper-surface pressures are shown since the distribution is antisymmetric. The motion considered is a rotation about the midchord point. The agreement between the present method and the method of Ref. 5 is excellent for the real part, but deviates somewhat near the leading edge for the imaginary part. The reason for this discrepancy has not been discovered.

A method for determining the pressures on a body undergoing arbitrary motion is described in Ref. 6. Since it is a nonlinear method, the steady and unsteady contributions to the pressure distribution are not treated separately as is done here. In order to make a comparison with the present method, a very small amplitude of motion must be used for the nonlinear calculation. The result is a very small unsteady contribution to the pressure. This small contribution is obtained by subtracting the steady pressure distribution from the complete pressure distribution (steady plus unsteady). Since the small unsteady pressure is then the difference between two large numbers, it may not be very accurate. In this respect, the nonlinear method is not particularly well suited to small-amplitude calculations. Also, the nonlinear method takes a transient approach to the problem; that is, all motions are treated as starting from rest. As a result, some starting transients are always present in a calculation meant to simulate simple-harmonic motion.

In spite of those objections, however, comparisons are attempted. The first example is presented in Fig. 4a). Specifically, a 25.5-%-thick Joukowski airfoil is made to pitch about its quarter-chord point at a reduced frequency of 0.628 and with an amplitude of 0.001 radians. (The amplitude of vibration is used only by the methods of Refs. 6 and 7.) Only the upper-surface pressure distributions are shown since the distributions are antisymmetrical. The agreement between the two methods is good. The complex lift as calculated by the present method is $-4.463 - i\,0.654$, whereas that calculated by the method of Ref. 6 is $-4.77 - i\,0.80$. A measure of the transient residue still present in the nonlinear calculation is the average lift, which for pure simple-harmonic motion is zero. In the example presented in Fig. 4a), the average lift at the time the pressures were determined was 3.5 percent of the amplitude of the unsteady lift. Some peculiarities can be seen in the pressure distribution at the trailing edge. These are caused by a slight thickening of the trailing edge that was used. This trailing edge was selected due to difficulties in dealing with a cusp trailing edge.

The second example is presented in Fig. 4b. The only difference between this case and that of Fig. 4a is that, here, the mean angle of attack of the airfoil is 45°, and the amplitude of vibration is 0.05 radians. The comparison between the present method and the method of Ref. 6 is not as good as that presented in Fig. 4a. This is due to the fact that simple-harmonic motion has not been achieved. Specifically, the average lift coefficient at the time the pressures were determined was 1.67π, whereas the steady value is 1.68π. The difference between these two values (0.03) seems small. However, in relation to the amplitude of the unsteady component of the lift (0.15) it is large (20 percent).

The actual value of the lift coefficient per unit amplitude is obtained by dividing the lift coefficient by the amplitude (in

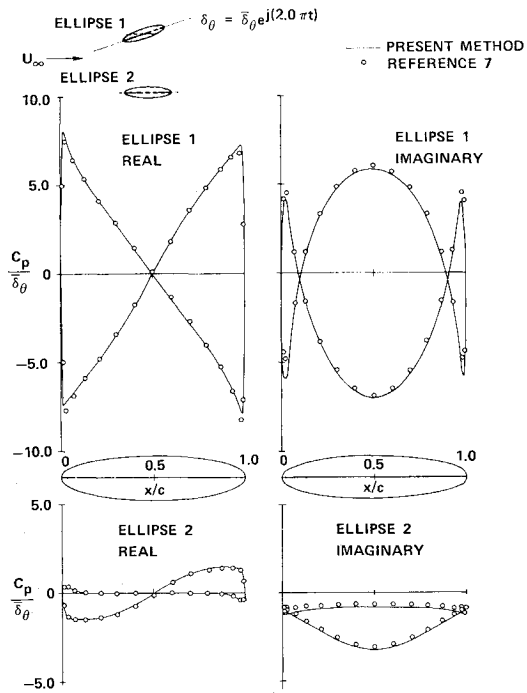

Fig. 5 Comparison of the pressure distributions as calculated by the present method and the method of Ref. 7 for two 25% thick ellipses in quasi-steady motion.

this case 0.05 radians). The pressure distributions are obtained by subtracting the steady values of the pressure from the unsteady values. Ideally, the average values should be used instead of the steady values, but they are not available. The average values of lift coefficient are available, however. When these average values are used in place of the steady values, better agreement between the present method and the method of Ref. 6 is realized. For example, the present method predicts a complex lift coefficient of $-2.60 - i\ 0.78$, whereas the method of Ref. 6 gives $-3.6 - i\ 0.62$ when steady values are used, and $-3.0 + i\ 0.0$ when average values are used.

Two-Body Cases

Reference 7 describes an extension of Ref. 6 whereby the nonlinear interaction of two bodies in unsteady motion is considered. Again, this method has the same disadvantages in relation to small-amplitude simple-harmonic motions, as does the method of Ref. 6. Despite the disadvantages, pressure-distribution comparisons are made. Figure 5 presents a comparison of the pressure distribution on two 25-%-thick ellipses as obtained by the present method and by the method of Ref. 7. The two ellipses are separated by a vertical distance of 1.5c, and the upper ellipse is made to vibrate in rotation about its center with a reduced frequency of 4. (For the method of Ref. 7, the amplitude of rotation is 0.05 rad.) In this special case, the ellipses cannot maintain circulation and thus shed no vortex wakes. The motion is therefore quasi-steady. This case is presented to illustrate the correctness of the quasi-steady boundary condition formulation without the complication of shedding wakes. Since the ellipses are nonlifting and noncirculatory, starting transients do not appear. Agreement between the two methods is very good and shows the desired result.

Figure 6 presents a second comparison with the method of Ref. 7. Specifically, the pressure distributions on two 25.5% thick Joukowski airfoils are shown. The vertical and horizontal distances between the two lifting airfoils is 0.50c and 0.25c, respectively. The upper airfoil is vibrating in rotation about its one-quarter-chord point with a reduced frequency of 0.2π, while the lower airfoil is stationary. The agreement between the two methods is consistent with that observed in Fig. 4a and Fig. 4b. The lift coefficients obtained by the present method are $-6.00 - i\ 1.10$ for the upper body and $3.12 - i\ 0.75$ for the lower one. The lift coefficients obtained using the method of Ref. 7 are $-6.54 - i\ 0.75$ and $3.82 - i\ 0.70$, respectively.

It is worth noting that the out-of-phase (imaginary) component is small compared to the in-phase (real) component. Under these circumstances, very small errors in phase angle can cause what appear to be large errors (at least on a percentage basis) in the imaginary parts.

Figure 7 is included in this section to present a practical example of a two-body case. The flap of a NACA 23012 airfoil is made to vibrate in rotation about an equilibrium incidence of 45°. The figure presents the configuration as well as the resulting pressure distribution. The complex lift coefficients for the main airfoil and flap are $-1.50 + i\ 0.18$ and $-0.588 - i\ 0.18$, respectively.

Gust Cases

The Sears function $\phi(k)$, where $k = \omega/2$ gives the complex lift response of a flat plate in a simple-harmonic gust field, specifically, $C_l = C_{l_a}\phi(k)$. Figure 8 shows a vector diagram of this function as given in Ref. 13. Reference 14 shows that the complex nature of the function at high frequencies can be eliminated simply by moving the gust reference conditions from the midchord to the plate leading edge. The resulting function $H(k)$, which is also shown in Figure 8, is related to

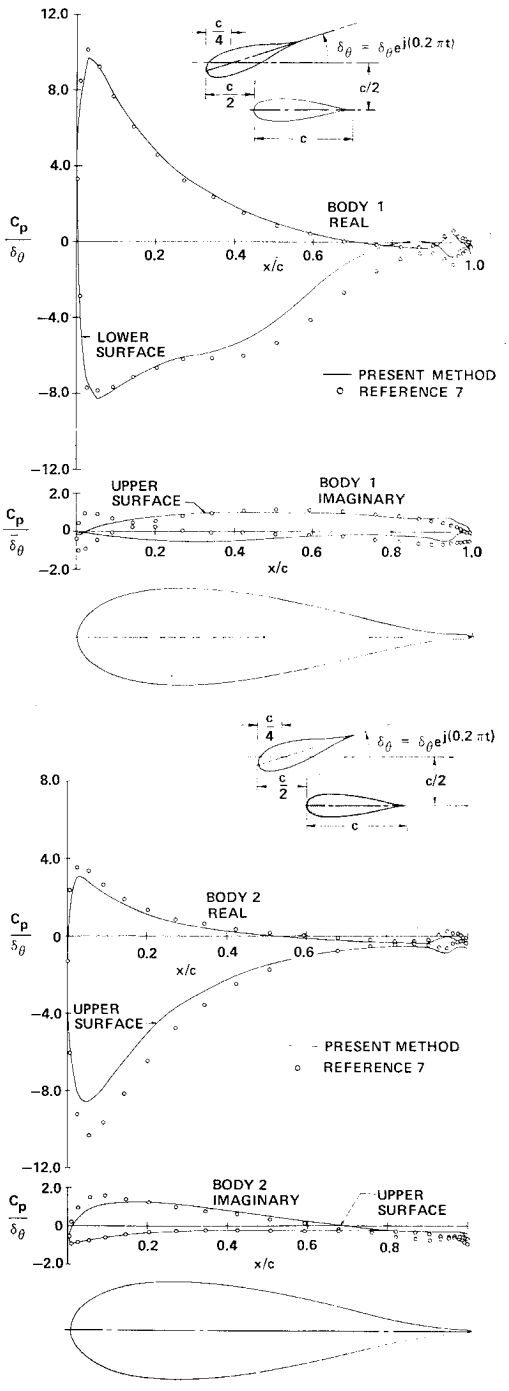

Fig. 6 Comparison of the pressure distributions as calculated by the present method and the method of Ref. 7 for two 25.5% thick Joukowski airfoils.

the Sears function $\phi(k)$ as follows:

$$\phi(k) = H(k)e^{ik}$$

The $H(k)$ function for a flat plate in a moving gust is also shown in Fig. 8. This function was obtained by applying a Fourier transformation to the results obtained in Ref. 15 for a moving sharp-edged gust. Specifically, a gust advancing toward the plate with a relative velocity of $2\ U_\infty$, i.e., $U_T = 2.0$, is considered. In the comparisons to follow, only $H(k)$, the simplified Sears function, will be considered. In addition, plots of these functions vs k will replace the vector diagrams.

Figure 9 presents the amplitude and phase angle of the simplified Sears gust function, $H(k)$. The results of calculations by the present method are also shown for a 4.2-percent-thick von Mises airfoil and a 25.5% thick Joukowski airfoil.

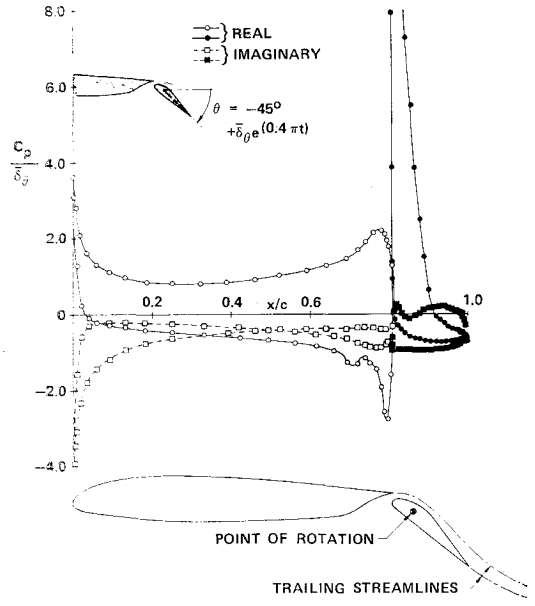

Fig. 7 Pressure distributions on a NACA 23012 airfoil and flap.

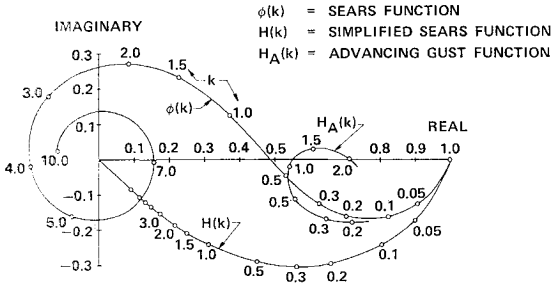

Fig. 8 Vector diagram of the Sears function, simplified Sears function, and the advancing gust function.

The results for the thin von Mises airfoil agree very well with the flat-plate results. The trends shown for the thickness are similar to those for the Theodorsen function (Fig. 2). The thickness tends to decrease the amplitude and increase the magnitude of the phase angle in both cases, except at high frequencies. There, the trend reverses for the phase angle.

Figure 10 presents the amplitude and phase angle of the simplified gust function for a plate in an advancing gust field.

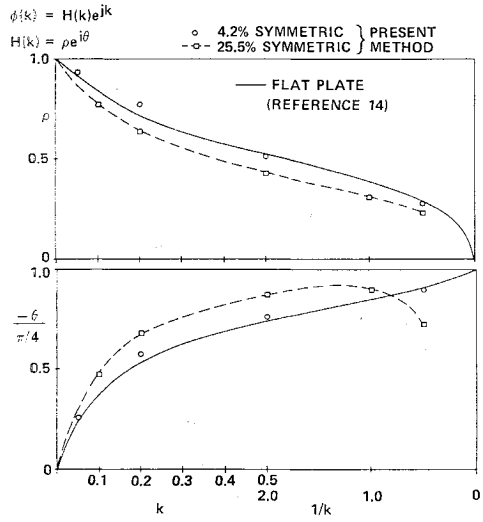

Fig. 9 Comparison of the simplified Sears function for airfoils of various thickness.

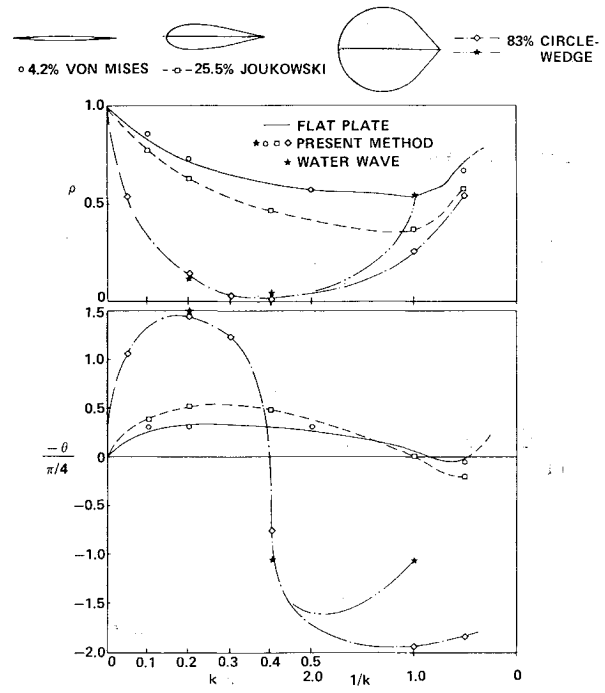

Fig. 10 Comparison of the advancing gust function for bodies of various thickness.

The plate is traveling to the left with a velocity of U_∞ and the gust is traveling to the right with a velocity of U_∞. The relative velocity is then $2U_\infty$, i.e., $U_T = 2.0$. The results of calculations by the present method are also shown for three different body shapes. The first is a 4.2-percent-thick von Mises airfoil, the second is a 25.5% thick Joukowski airfoil, and the third is an 83-percent-thick circle-wedge type of body. The results for the thin airfoil agree very well with those for the flat plate. The calculations for the thick Joukowski airfoil show the same thickness trends that were observed for the stationary gust. The extremely thick circle-wedge body confirms these trends.

Calculations were also carried out for the circle-wedge body in a water-wave gust field with $U_T = 2.0$. The results (indicated by stars in Fig. 10) are normalized by the quantity §§$\omega(1 - U_T)/U_T e^{\omega y_{ave}/U_T}$. For low values of reduced frequency, the water-wave gust and the advancing gust are almost identical. This is due to the fact that the onset flows for the two types of gusts are very nearly the same for low frequencies (when the results are normalized as given above). At higher frequencies, the exponential character of the wave onset flow makes itself felt, and in this range the results differ.

References

[1] Fung, Y. C., *An Introduction to the Theory of Aeroelasticity*, Wiley, New York, 1955, pp. 395–417.

[2] Woods, L. C., "The Lift and Moment Acting on a Thick Aerofoil in Unsteady Motion," *Royal Society of London Philosophical Transactions*, Vol. 247, No. A925, Nov. 1954.

[3] Kussner, H. G. and Gorup, G. V., "Instationäre linearisierte Theorie der Flugelprofile endlicher Dicke in kompressibler Strömung," *Mitteilungen des Max-Planck-Institut für Stromungsforschung an der Aerodynamischen Versuchsanstalt*, Nr. 26, Gottingen, 1960.

[4] Hewson-Browne, R. C., "The Oscillation of a Thick Aerofoil in an Incompressible Flow," *Mechanics and Applied Mathematics*, Vol. XVI, Feb. 1963.

[5] Van De Vooren, A. I. and Van De Vel, H., "Unsteady Profile Theory in Incompressible Flow," *Archiwum Mechaniki Stosowanej 3*, Vol. 16, 1964.

§§ y_{ave} is the depth of the average chord line of the body.

[6] Giesing, J. P., "Nonlinear Two-Dimensional Unsteady Potential Flow with Lift," *Journal of Aircraft*, Vol. 5, No. 2, March–April 1968, pp. 135–143.

[7] Giesing, J. P., "Nonlinear Interaction of Two Lifting Bodies in Arbitrary Unsteady Motion," *Transactions of ASME*, Ser. D; *Journal of Basic Engineering*, Vol. 90, No. 3, Sept. 1968.

[8] Djojodihardjo, R. H. and Widnall, S. E., "A Numerical Method for the Calculation of Nonlinear, Unsteady Lifting Potential Flow Problems," *AIAA Journal*, Vol. 7, No. 10, Oct. 1969.

[9] Milne-Thompson, L. M., *Theoretical Hydrodynamics*, Macmillan Co., New York, 1960.

[10] Giesing, J. P., "Potential Flow About Two-Dimensional Airfoils," LB39146, 1965, Douglas Aircraft Co.

[11] Giesing, J. P., "Two-Dimensional Potential Flow Theory for Multiple Bodies in Small-Amplitude Motion," DAC 67028, April 1968, McDonnell Douglas Aircraft Co.

[12] Giesing, J. P., "Vorticity and Kutta Condition for Unsteady Multi-Energy Flows," *Transactions of ASME*, Ser. E, *Journal of Applied Mechanics*, Vol. 36, No. 3, Sept. 1969.

[13] Sears, W. R., "Some Aspects of Non-Stationary Airofoil Theory and Its Practical Application," *Journal of Aerospace Sciences*, Vol. 8, No. 3, 1941, pp. 104–108.

[14] Giesing, J. P., Rodden, W. P., Stahl, B., "The Sears Function and Lifting Surface Theory for Harmonic Gust Fields," *Journal of Aircraft*, Vol. 7, No. 3 May-June 1970 pp. 252–255.

[15] Drischler, J. A., Diederich, F. W., "Lift and Moment Responses to Penetration of Sharp-Edged Traveling Gusts, with Application to Penetration of Weak Blast Waves," TN 3956, May 1957, NACA.

NOVEMBER 1970 AIAA JOURNAL VOL. 8, NO. 11

Results from a New Wind-Tunnel Apparatus for Studying Coning and Spinning Motions of Bodies of Revolution

LEWIS B. SCHIFF* AND MURRAY TOBAK*
NASA Ames Research Center, Moffett Field, Calif.

An apparatus is described which reproduces either separate or combined coning and spinning motions of a body of revolution in a wind tunnel, using a six-component strain gage balance to measure the aerodynamic forces and moments. Results of experiments with a slender cone in coning motion show that at small angles of attack the side-force and side-moment coefficients normalized by the coning rate are linear functions of the angle of attack, the slopes of which are in excellent agreement with the damping-in-pitch coefficients $C_{N_q} + C_{N\dot{\alpha}}$ and $C_{m_q} + C_{m\dot{\alpha}}$. This agreement, predicted by linearized theory, indicates that at small angles of attack the dynamic damping-in-pitch coefficients of a body of revolution can be measured as the steady side force and moment coefficients of the body undergoing coning motion. For larger angles of attack, where vortices appear on the leeside of the body, the normalized side force and moment coefficients become nonlinear functions of angle of attack. Photographs of the vortices reveal that they are displaced from the angle-of-attack plane by coning motion. This asymmetric displacement of the vortices persists over the entire length of the body, making them a possible source of nonlinear side moment.

Nomenclature

A = axial force (Fig. 1)
C_l = rolling-moment coefficient, l/q_0Sl_0
C_m = pitching-moment coefficient, m/q_0Sl_0
C_{m_v} = that contribution to the pitching-moment coefficient attributable to the presence of vortices
C_n = side-moment coefficient, n/q_0Sl_0
$C_{np\alpha}$ = rate of change of linearized side-moment coefficient with respect to p and α; $[\partial^2 C_n/\partial(pl_0/V_0)\partial]_{\substack{\alpha\alpha\to 0\\ p\to 0}}$; classical Magnus moment coefficient
C_N = normal-force coefficient, N/q_0S
C_{N_v} = that contribution to the normal-force coefficient attributable to the presence of vortices
$C_{N\alpha}, C_{m\alpha}$ = rate of change of linearized normal-force and pitching-moment coefficients with angle of attack; $(\partial C_N/\partial\alpha)_{\alpha\to 0}$, $(\partial C_m/\partial\alpha)_{\alpha\to 0}$
C_{N_q}, C_{m_q} = rate of change of linearized normal-force and pitching-moment coefficients with pitching velocity parameter ql_0/V_0; $[\partial C_N/\partial(ql_0/V_0)]_{q\to 0}$, $[\partial C_m/\partial(ql_0/V_0)]_{q\to 0}$
$C_{N\dot{\alpha}}, C_{m\dot{\alpha}}$ = rate of change of linearized normal force and pitching-moment coefficients with time rate of change of angle-of-attack parameter $\dot{\alpha}l_0/V_0$ $[\partial C_N/\partial(\dot{\alpha}l_0/V_0)]_{\dot{\alpha}\to 0}$, $[\partial C_m/\partial(\dot{\alpha}l_0/V_0)]_{\dot{\alpha}\to 0}$
$C_m\{\infty;\sigma(t),0,0\}$ = pitching-moment coefficient in steady planar motion with σ held fixed at $\sigma(t)$; zeroes denote ϕ and ψ respectively held fixed at zero
$C_{m_{\dot{\sigma}}}\{\sigma(t),0,0\}$ = damping-in-pitch coefficient in planar motion (ϕ and ψ held fixed at zero) measured about a fixed inclination σ = const
$C_{n\dot{\phi}}\{\infty;\sigma(t),0,0\}$ = rate of change with respect to coning rate parameter $\dot{\phi}l_0/V_0$ of the side-moment coefficient measured in steady coning motion (with σ held fixed at $\sigma(t)$, $\dot{\phi}$ held fixed at a series of values, and ψ held fixed at zero), evaluated at $\dot{\phi} = 0$
$C_{n\dot{\psi}}\{\infty;\sigma(t),0,0\}$ = rate of change with respect to spin rate parameter $\dot{\psi}l_0/V_0$ of the side-moment coefficient measured in steady spinning motion (with σ held fixed at $\sigma(t)$, ψ held fixed at a series of values, and ϕ held fixed at zero), evaluated at $\dot{\psi} = 0$
C_Y = side-force coefficient, Y/q_0S
l_{cg} = length along body axis of symmetry from nose to center of rotation (Fig. 2)

Received February 20, 1970; revision received May 11, 1970.
* Research Scientist. Member AIAA.